REPORT DOCUMENTATION PAGE

AFRL-SR-BL-TR-01-

0400

Public reporting burden for this collection of information is estimated to average 1 hour per response, including the tim
gathering and maintaining the data needed, and completing and reviewing the collection of information. Send comme
collection of information, including suggestions for reducing this burden, to Washington Headquarters Services, Directo
Davis Highway, Suite 1204, Arlington, VA 22202-4302, and to the Office of Management and Budget, Paperwork Reduction Project (0704-0188) Washington, DC 20503

1. AGENCY USE ONLY (Leave Blank)	2. REPORT DATE	3. REPORT TYPE AND DATES COVERED
	December 30, 2000	Final Report; October 1, 1997 – September 30, 2000

4. TITLE AND SUBTITLE	3. FUNDING NUMBERS
Mechanism for Solid State Crystal Conversion	F49620-98-C-0002

6. AUTHORS
Charles D. Greskovich and James A. Brewer

7. PERFORMING ORGANIZATION NAME(S) AND ADDRESS(ES)
GE Corporate Research and Development, 1 Research Circle, Niskayuna, NY 12309

8. PERFORMING ORGANIZATION REPORT NUMBER
2000SRD005

9. SPONSORING / MONITORING AGENCY NAME(S) AND ADDRESS(ES)
Air Force Office of Scientific Research, Directorate of Aerospace and Materials Science
801 North Randolph Street, Mail Room 732
Arlington, VA 22203-1977

10. SPONSORING / MONITORING AGENCY REPORT NUMBER

11. SUPPLEMENTARY NOTES

AIR FORCE OFFICE OF SCIENTIFIC RESEARCH (AFOSR)
NOTICE OF TRANSMITTAL DTIC. THIS TECHNICAL REPORT
HAS BEEN REVIEWED AND IS APPROVED FOR PUBLIC RELEASE
LAW AFR 190-12. DISTRIBUTION IS UNLIMITED.

12a. DISTRIBUTION / AVAILABILITY STATEMENT
Approved for public release; distribution is unlimited

12b. DISTRIBUTION CODE

13. ABSTRACT (Maximum 200 words)
A MgO-depletion mechanism is proposed for the Solid State Crystal Conversion (SSCC) phenomenon in MgO-doped Al_2O_3, where sapphire crystals grew up to 5 cm in length by classical abnormal grain growth in microstructures with average grain sizes of 10-45 microns. When the MgO concentration decreased (via evaporation) at temperatures between ~1750 and 1900°C and reached a critical concentration (C_{MgO}-Crit.) of ~ 60ppm, an abnormal grain suddenly "nucleated" and migrated through the polycrystalline matrix at velocities 1000-fold higher. Above C_{MgO}-Crit., charged Mg^{2+} ions and oxygen vacancies apparently interacted strongly with grain boundaries. Near C_{MgO}-Crit. the sudden, 1000-fold rise in grain boundary diffusion indicated weak grain boundary/solute interaction. This phenomenon was related to possibly (a) charge compensation of Mg^{2+} by Si^{4+}-impurity and/or (b) a "non-blocking" phenomenon, whereby Mg^{2+} ions no longer impede grain growth by occupying kink sites on grain boundary steps. Large single crystals grew with irregular growth fronts moving at velocities of 4 microns per second (1.5 cm/h) with their c-axis oriented primarily ~ 90° or 45° to the tube axis. TEM lattice images of growth fronts showed clean crystal boundaries with no liquid phase or film.

14. SUBJECT TERMS	15. NUMBER OF PAGES
MgO-depletion mechanism of crystal growth in Al_2O_3, controlled MgO concentration, high grain boundary mobilities near intrinsic values, sintering/grain growth, tubular crystal orientations	33
	16. PRICE CODE

17. SECURITY CLASSIFICATION OF REPORT	18. SECURITY CLASSIFICATION OF THIS PAGE	19. SECURITY CLASSIFICATION OF ABSTRACT	20. LIMITATION OF ABSTRACT
unclassified	unclassified	unclassified	UL

Mechanism for Solid State Crystal Conversion

Final Report: October 1, 1997 – September 30, 2000

Contract F49620-98-C-0002, Grant 204584

Prepared by

Charles D. Greskovich and James A. Brewer
GE Corporate Research and Development
1 Research Circle
Niskayuna, NY 12309

Prepared for

Air Force Office of Scientific Research
Directorate of Aerospace and Materials Science
801 N. Randolph Street, Mail Room 732
Arlington, VA 22203-1977

December 30, 2000

20010711 079

Table of Contents

Executive Summary

The mechanism of Solid State Crystal Conversion (SSCC) was investigated for converting dense tubes of polycrystalline, MgO doped alumina (PCA) into single crystal sapphire at temperatures 100-300°C below the melting point. Sapphire crystals were observed to grow up to 5 cm in length by classical abnormal grain growth (AGG). The concentration of MgO in the Al_2O_3 solid solution dominated the SSCC event under all circumstances. During high-temperature grain growth, the concentration of MgO in the sample continuously decreased by MgO evaporation. When the C_{MgO} approached a critical MgO concentration, C_{MgO}-Crit., of ~ 60 ppm, one or more abnormal grains "nucleated" in the MgO-depleted region(s) and grew suddenly to lengths of several centimeters along the tubes. This condition held true for samples prepared with powders with different purity, co-doped with several hundred ppm of Cr_2O_3 or Ti_2O_3, and sintered under isothermal or temperature gradient conditions. The C_{MgO}-Crit was measured to be well within the solubility limit for MgO in Al_2O_3. The large tubular crystals grew with their c-axis oriented primarily ~90° or 45° to the tube axis. High-resolution lattice imaging of several SC/PCA interfaces showed only clean crystal boundaries with no evidence whatsoever for any liquid phase or film.

The average migration velocity (V) of the single-crystal was very high, reached ~ 4 microns per second (1.5 cm/h) at temperatures above 1700°C and agreed well with intrinsic velocities and mobilities predicted for "pure" Al_2O_3. This was the first time experimental mobilities for grain boundary migration approached the predicted, intrinsic mobilities for a ceramic oxide material.

A MgO-depletion mechanism explained the SSCC phenomenon in MgO-doped Al_2O_3. The decreasing MgO concentration occurred via evaporation, and once the average MgO solute concentration in the sample reached C_{MgO}-Crit., an abnormally large grain suddenly "nucleated" and migrated with a velocity 1000-fold higher. Above C_{MgO}-Crit., charged Mg^{2+} ions and oxygen vacancies interacted strongly with grain boundaries, possibly by electric field (space charge) effects. The sudden rise in grain boundary diffusion by 1000-fold near or at C_{MgO}-Crit. may be related to charge compensation of Mg^{2+} by Si^{4+}. Alternatively, the 1000-fold rise in grain boundary diffusion (and mobility) could be caused by a "non-blocking" phenomenon whereby Mg^{2+} ions no longer impede grain growth by occupying kink sites on grain boundary steps responsible for grain boundary migration.

This research work also resulted in the MS Thesis of Harold Gholston in the Materials Department at Northwestern University, a manuscript on "The Solubility of MgO in Al_2O_3 at High Temperatures," accepted for publication in the *Journal of the American Ceramic Society*, and a patent application, "Conversion of Polycrystalline Al_2O_3 to Single Crystal Sapphire."

1. Introduction and Background

The unique properties of many single crystals provide great benefits in a wide range of magnetic, structural, optical and other applications. Unfortunately, the high cost of producing and machining single crystals into desirable shapes and sizes often precludes their use in many applications. For example, single crystal sapphire could find extensive use as transparent armor if it could be produced economically in large sizes and shapes[1]. If a low-cost process could be found for converting dense, polycrystalline ceramics of complex shape into single crystals at temperatures well below the melting point (i. e., during the sintering/grain growth process), then single crystals with complex compositions and crystal structures would find wider applications.

There have been several investigations related to growth of large single crystals from dense polycrystalline materials. In 1985 Tanji et al.[2] reported a solid-solid process for producing Mn-Zn ferrite single crystals. The ferrite method required bringing a polished seed crystal into direct contact with a dense, fine-grain sintered body and heating to temperatures between 1350 and 1400°C. The rate of growth of the ferrite crystal into the polycrystalline body was relatively slow, only a few millimeters per hour. A similar technique was used to grow a seed crystal of Yttrium-Iron-Garnet (YIG) into a polycrystalline body of the same composition at 1500°C in oxygen[3]. After 8 hours of solid state reaction the YIG crystal grew about 5 mm into the polycrystalline matrix. Yoo et al.[4] demonstrated the growth of $BaTiO_3$ single crystals by using the abnormal grain growth method. In this case a very small amount of SiO_2 impurity was placed on top of a $BaTiO_3$ powder compact to form seed grains. The seed grains continued to grow at 1370°C into single crystals with sizes up to a few centimeters. The rate of crystal boundary migration in the $BaTiO_3$ samples was measured as ~ 0.2 mm per hour. In 1997 the authors reported[5] growth of long (~10 cm) sapphire crystals in dense MgO-doped Al_2O_3 tubes by a new process named Solid State Crystal Conversion (SSCC). In this method dense, translucent, MgO-doped polycrystalline Al_2O_3 (PCA) could be converted into sapphire at a temperature of 1880°C in a reducing atmosphere, nearly 200°C below the melting. Some processing parameters such as powder purity and sintering temperature, time and atmosphere were investigated in a cursory fashion to determine the degree of conversion of PCA into sapphire crystals. The SSCC event was enhanced by the addition of several hundred ppm of Cr_2O_3 or Ga_2O_3 to MgO-doped (650 ppm) Al_2O_3. Typically, one or more large (cm-size) alumina crystals developed on the open ends of a sintered tube with lengths up to 15 cm occasionally grew with the c-axis oriented perpendicular to the tube axis. The growth of a small number of sapphire crystals was correlated with residual MgO concentrations – <60 ppm in the converted samples. The migration velocity for crystal boundary movement through the PCA matrix was experimentally measured to be about 1 cm/h at 188°C, a very high value that was close to the intrinsic value expected for grain boundary migration in "pure" alumina. The rate of abnormal grain growth in alumina was at least about a factor of 10 greater than those observed in Mn-Zn ferrite, YIG and $BaTiO_3$. It would be very useful to understand the practical and theoretical aspects of growing cm-size sapphire crystals from PCA ceramic.

Sintered PCA is a practical starting material for investigating the SSCC event because it has a desirable microstructure in which abnormal grain growth can be eventually stimulated under certain conditions. Translucent PCA is produced from relatively high purity (≥99.98%), de-agglomerated alumina powder with specific surface areas of 5-30 m^2g^{-1}. Typically, 500 to 750 ppm of MgO is mixed into the powder in order to act as an inhibitor to abnormal grain growth during the sintering step. Abnormal grain growth must be prevented during final stage sintering in order to eliminate the last few

percent of closed pores residing on the grain boundaries. Green compacts in tubular form are fabricated by extrusion or isostatic-pressing followed by a binder burnout cycle in air at 800-1000°C. The powder compacts are then sintered in a hydrogen atmosphere at temperatures near 1850°C for a few hours and undergo ~20% linear shrinkage as the porosity decreases from ~50% to nearly zero. The residual porosity becomes very low, usually 5×10^{-4} to 1×10^{-4}, and the sample is optically translucent. The microstructure is also characterized by a uniform distribution of grains of average size ~25-30 microns and a small volume fraction (<1%) of spinel ($MgAl_2O_4$) particles 0.3 to 3 microns in size located at 3- and 4-grain intersections. There is no evidence of any residual liquid phase arising from impurities (Si, K, Na, Ga) in the starting alumina powder. This is probably because most impurities, including a large portion of the MgO additive, evaporate in the hydrogen (reducing) atmosphere. The final microstructure of translucent PCA contains very little solid second phase, porosity and adverse impurities that can cause a drag or retarding force on a moving grain boundary. If the MgO concentration in the sample can be further reduced by evaporation during extended sintering, abnormal grain growth can "nucleate" and proceed at very high rates.

Determination of the temperature region where abnormal grain growth proceeds in fully dense, MgO-doped Al_2O_3 is critically important for the SSCC process. For initiation of abnormal grain growth, a grain boundary must reach a condition of "breakaway" from the various drag forces inhibiting its movement. Because the mobility of a grain boundary is exponentially dependent on temperature, high temperatures will have a large effect on promoting abnormal grain growth. Burke et.al.[6] reported the growth of large surface grains of Al_2O_3, several mm wide and only ~40 microns thick, on samples of MgO-doped Al_2O_3 sintered for 3 hours in hydrogen gas at 1880°C. They explained that abnormal growth of large surface grains probably initiated when the MgO concentration decreased due to evaporation from the external surfaces of the sample. Based on the sizes of the surface grains, the velocities for lateral growth and "depth-growth" were estimated to be $\sim 3 \times 10^{-5}$ cm/s and $\sim 3 \times 10^{-7}$ cm/s, respectively. Since the lateral growth velocity of the surface grains corresponded to 1.1 mm per hour, we attempted to grow cm-size sapphire crystals during the sintering process at temperatures near 1900°C.

2. Objectives and Approach

The current AFOSR program entitled "Mechanism for Solid State Crystal Conversion" involved performing well-controlled, grain growth and chemical doping experiments in sintered MgO-doped Al_2O_3. The intent was to explore this system as a possible model material for providing unambiguous evidence about the mechanism(s) of high-velocity, abnormal growth of cm-size (single-crystal like) grains in dense polycrystalline matrices. The overall objective was to gain understanding of the ceramic materials/chemistry/physics phenomena leading to the "nucleation event(s)" and growth of one or more grain-growth sites. A further objective was to determine if a proposed mechanism based on "MgO-Depletion" from a specific region(s) of the PCA sample was responsible for movement of abnormal grain boundaries with extraordinarily high velocities.

The research work included selecting two Al_2O_3 powders of different purity for sample preparation and establishing a reliable method for uniformly mixing appropriate levels of selected co-dopants (Cr_2O_3, Ti_2O_3 and Mo) into the starting powders or the bisque-fired tubes already doped with MgO. Sintering and grain growth experiments were conducted to assess the effect of lower (<350 ppm) initial

MgO concentration on accelerating the PCA-to-sapphire conversion. In some cases powder compacts with low MgO compositions were sintered and then hot-isostatic-pressed to produce nearly pore-free microstructures for subsequent investigation of abnormal grain growth. It was also necessary to measure the solubility limits of MgO in Al_2O_3 at temperatures between 1700 and 2000°C to obtain basic understanding of the important role that MgO solubility has on grain boundary mobility. The effects of sintering temperature and temperature gradient on the SSCC process were studied. The orientation and surface topography of some of the grown crystals were also measured. The velocities and mobilities for grain boundary migration were measured, and a mechanism of MgO-depletion proposed for abnormal growth of cm-size crystals in MgO-doped PCA ceramic.

3. Experimental Procedures

3.1 Powder Preparation and Processing

Two types of high-purity Al_2O_3 powders were used to understand the effect of material purity on the PCA-to-sapphire conversion. One powder was Baikowski CR-10, which was commercially available and characterized by having a purity of 99.98%, median particle size of 0.31 μm and specific surface area of 8.8 m^2/g. The second powder was Sumitomo AA-05, which had a higher purity of 99.99%, median particle size of 0.52 μm and specific surface area of 3.2 m^2/g. The particle size distributions of both alumina powders showed that no agglomerates were greater than 2 μm in size.

A number of extrusion batches were prepared from both alumina powders with different MgO concentrations (Table 1). A typical batch was prepared by mixing 2000 g of alumina powder with an appropriate amount of binder, lubricant and magnesium nitrate. Each powder batch was extruded into tubing with approximate dimensions 6.8 mm o.d., 6.1 mm i.d. and 0.7 mm wall thickness. The best results for optimum extruded material occurred when the extrusion pressure was ~152 MPa for the Baikowski mix and ~90 MPa for the Sumitomo mix. Three hundred centimetrers of tubing was extruded, dried at ~ 100°C and then bisque-fired at 1050°C in air for binder/lubricant removal. The green density of the bisque-fired tubes was measured by Archimedes' method in water and was about 1.92 g/cm^3.

Table 1. Extrusion batches of alumina powder doped with various initial MgO concentrations.

Batch No.	Powder Type	MgO Content (ppm)
1	Baikowski CR-10	350
2	Baikowski CR-10	120
3	Baikowski CR-10	0
4	Sumitomo AA-05	350
5	Sumitomo AA-05	0

3.2 Preparation of MgO and Codopant Compositions in Bisque-Fired Tubes via Liquid Immersion Method

For investigating the MgO solubility in Al_2O_3 at high temperatures, Batch No. 5 Sumitomo material was doped with MgO concentrations ranging from 0 to 300 ppm by a liquid immersion method. A series of bisque-fired Sumitomo AA-05 tubes were carefully immersed in aqueous stock solutions containing different magnesium nitrate concentrations that would produce MgO-doping levels ranging from 0 to 300 ppm at 50 ppm intervals. The following equation was derived and applied.

$$W_d/W_i\ (PPM) = [(W_s - W_i)/ W_i]\ (C_d \times 10^6/ D_s) \qquad (1)$$

W_d is the weight of magnesium nitrate solution absorbed by a porous sample, W_i is the initial dry weight of the sample, W_s is the saturated sample weight, C_d is the concentration of the magnesium nitrate solution in g/ml, and D_s is the density of the magnesium nitrate solution in g/ml (~1 g/ml). If the saturated sample weight, dry weight, solution density and desired magnesium nitrate concentration in the sample are known, then the concentration of the magnesium nitrate solution is specified and can be prepared as an aqueous stock solution. Table 2 lists the concentration of Mg-nitrate and corresponding MgO required to dope porous alumina samples by the liquid immersion technique. A typical doping procedure involved soaking bisque-fired tubes, each weighing ~ 3 g, for 3 minutes in each dopant solution while under vacuum, removing and drying-off the excess free liquid from the sample surfaces, and freeze-drying the soaked samples to prevent dopant segregation upon water sublimation. The Mg-doped samples were then sintered to relative densities of 95.6 to 96.1 % (the closed pore state) in air at 1600°C for 2h to ensure complete MgO entrapment within each sample. The MgO concentrations in the fired samples were quantitatively measured by the ICP-AES method (see next section). The MgO concentrations in the fired samples were compared to the predicted MgO concentration from Equation (1) and plotted in Figure 1. The measured MgO concentrations are within ~7% of the predicted values, and the results suggest the liquid immersion technique is quite acceptable and convenient for doping porous compacts.

Other dopants studied for their effect on the SSCC process were Cr_2O_3, Ti_2O_3 and Mo. (The reduced forms of titanium oxide and molybdenum are mentioned because these dopants become reduced when fired in a hydrogen atmosphere during the SSCC process). The dopant concentrations evaluated were 100 and 200 ppm of Cr_2O_3 and Ti_2O_3, and 2-40 ppm of Mo. The source materials that

Table 2. The concentration of Mg-nitrate and MgO required for doping bisque-fired alumina samples by liquid immersion.

C_d Mg-nitrate, 10^{-3} g/ml	C_d MgO, 10^{-4} g/ml	W_d/W_i, ppm MgO
1.15	1.88	50
2.30	3.77	100
3.45	5.65	150
4.60	7.53	200
5.75	9.40	250
6.90	11.3	300

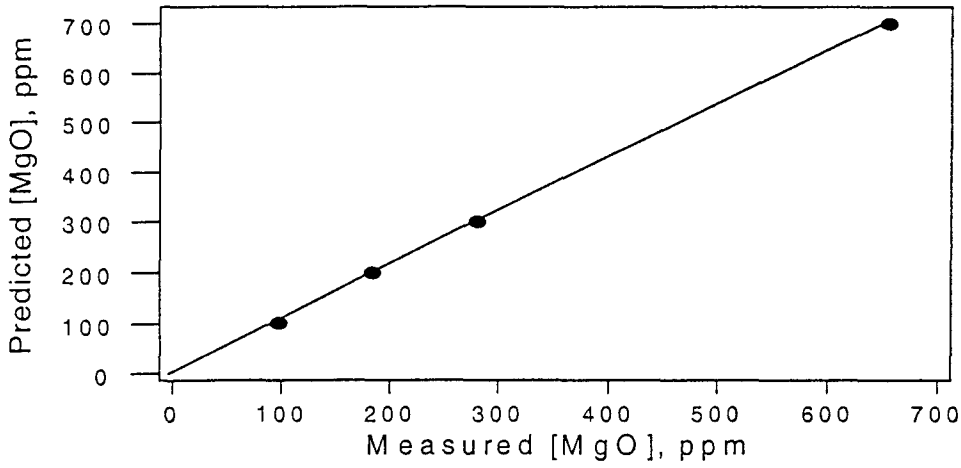

Figure 1. Predicted versus measured MgO contents in porous Al_2O_3 samples doped by liquid immersion.

were soluble in water were $CrCl_3 \cdot H_2O$ and molybdic acid. When doping with $CrCl_3$ solution a soak time not exceeding 3 minutes was necessary because of selective Cr^{3+} absorption on the surfaces of the Al_2O_3 particles. For example, if an alumina sample was soaked for 15 minutes in a $CrCl_3$ stock solution, the measured Cr_2O_3 in the fired sample was greater than 3X the predicted amount from Equation (1). For the case of the Ti-dopant the bisque-fired alumina tubes were soaked in a slightly acidified solution of isopropyl alcohol containing titanium isopropoxide, $Ti(OC_3H_7)_4$.

3.3 Chemical Analysis

The MgO and co-dopant concentrations were measured in many MgO-doped alumina compositions after being bisque-fired, prefired at 1600°C and sintered at various temperatures near and above 1700°C in hydrogen gas. The samples were analyzed using a Varian Liberty II ICP-AES instrument. Sample preparation involved carefully grinding the selected sample in a clean sapphire mortar and pestle to get the powder to pass through a 60-mesh nylon screen. Then 0.2 to 0.4 g of powdered sample was placed in an acid rinsed, Teflon insert and 1.5 ml of H_2SO_4 and 3.5 ml of H_3PO_4 were added. The Teflon insert was placed and sealed inside a microwave, high-pressure bomb and heated until the powder composition dissolved. After cooling, the solution was transferred into 25 ml volumetric flasks. An acid blank and spike were carried through the entire digestion procedure. The Varian II ICP-AES instrument was calibrated with 0, 0.02, 0.05, 0.1, 0.2, 0.5, and 1.0 ppm of Mg or Cr or Mo. The reported MgO and Cr_2O_3 values were accurate within ±5 ppm for the range investigated. The limit of detection for Mo was 8 ppm.

Electron microprobe and SEM methods were used for quantitative and qualitative chemical analysis of spinel second phase ($MgO \cdot n\ Al_2O_3$, where n is a small number >1) located primarily at 3-grain intersections in the microstructures of sintered MgO-doped Al_2O_3 compositions. In both cases a small electron beam was placed on the surface of a spinel particle 2-3 micron in average size and the Mg, Al and O x-ray signals detected by solid-state x-ray detectors.

3.4 Sintering/Grain Growth and Equilibration Experiments

Most sintering and grain growth experiments were carried out in a dedicated tungsten-mesh resistance furnace, having a hot zone 15 cm in diameter and 30 cm long, and capable of controlling temperatures up to 2200°C within ±10°C in hydrogen atmospheres with dew points ranging between approximately –40°C and +20°C. A typical sintering/grain growth experiment involved placing a bisque-fired tube or prefired tube, 5 to 10 cm in length, inside a slightly larger molybdenum tube, which in turn was placed inside a molybdenum box with a loose lid. The sample would be heated within 5h to a desired sintering temperature between 1700 and 2000°C, depending on the initial MgO concentration of the sample. Samples with initial MgO concentrations <200 ppm were generally sintered at temperatures below 1850°C, while higher MgO compositions were sintered up to 2000°C. The same applied for MgO-doped Al_2O_3 compositions with co-dopants. Unless specifically mentioned, the dew point of the hydrogen gas was generally +10°C. This dew point was equivalent to an oxygen partial pressure of $\sim 10^{-10}$ atm at 1850°C. Consequently, all sintering/grain growth runs were carried out under strongly reducing conditions. After just 1 or 2h of sintering time at temperatures between 1700 and 2000°C, the samples typically densified to various degrees of optical translucency. Soak times >2h were used primarily to cause grain growth and reduce the MgO concentration by evaporation in the reducing environment.

Some grain growth experiments were done in a temperature gradient by placing the "crucible" at the bottom end of the furnace hot zone. Here a tube-shaped sample was placed vertically in a vertical molybdenum tube supported in a molybdenum box. This sample orientation permitted a temperature gradient of about 60°C along the sample tube at average temperatures of 1800-1950°C. This experimental procedure usually resulted in abnormal grain growth initiating on the hot end of the dense tube.

A few grain growth experiments were done with Al_2O_3 samples containing <200 ppm of MgO that had been sintered and then hot-isostatically pressed in argon gas at 1600°C. These fine-grained and partially translucent samples were subsequently used to study the growth of cm-size sapphire crystals at the lowest temperatures investigated.

MgO-doped Al_2O_3 compositions, where the MgO concentration was increased by 50 ppm increments between 0 and 300 ppm, were equilibrated at 1700 to 2000°C to determine the solubility of MgO in Al_2O_3. To suppress MgO loss during equilibration at various temperatures, tubes of each composition were first sintered (shrunk) at 1600°C in oxygen and then inserted inside a green tube of the same MgO concentration. This technique was used to co-sinter and bond the outer tube onto the OD of the inner tube to further help prevent MgO evaporation from the surface of the inner tube during subsequent heating in the tungsten-resistance furnace. Samples of each composition were given a fast heating rate of ~1°C/s to the equilibration temperature, held for soak times of ½ to 5 h, depending on peak temperature, and then rapidly cooled at rates of ~10°C/s. This thermal cycle minimized MgO evaporation from the samples, ensured chemical equilibrium at temperature and avoided spinel precipitation during cooling.

Transverse sections of equilibrated samples with different compositions were cut with a diamond saw and relief-polished with sub-micron diamond paste to help reveal grain boundaries and any spinel particles in the microstructures. In compositions outside the MgO solubility limit at 1900 and 2000°C, the spinel particles were readily detected by SEM as ½ to 3 mm particles located at 3-grain intersec-

tions between large (20 to 50 mm) Al_2O_3 grains. Since the Al_2O_3 matrix grains were much smaller in sample compositions heated at 1720 and 1800°C, transverse sections had to be relief-polished and thermally etched for only a few minutes at 1550°C in air to clearly reveal grain boundary intersections (possible sites for the small spinel particles). If the thermal etching treatment occurred in moist hydrogen gas, no spinel particles were observed in any composition due to decomposition of spinel into Al_2O_3 and MgO gas. Fast heating and cooling rates of ~0.5°C/s were used to help prevent possible spinel precipitation during thermal etching.

The presence of a single-phase or two-phase mixture in each equilibrated sample was determined by SEM examination of the microstructure in the central region of the inner tube wall. Spinel (second phase), if present, was in the form of triangular-shaped particles located at 3- and 4-grain intersections. Consequently, typically 300 to 400 grain intersections were carefully examined in each sample for spinel particles by SEM at magnifications up to ~8000X. Absolute identification of a spinel-type particle was confirmed by semi-quantitative chemical analysis by placing the e-beam on the particle and detecting both Al and Mg peaks using energy dispersive x-ray spectroscopy. There was no Mg signal detected in any matrix grain of Al_2O_3 solid solution under the same conditions.

3.5 Characterization of Grain Growth in MgO-and Codoped-Al_2O_3 Samples

The extent of abnormal grain growth in fired sample compositions was frequently assessed by using optical microscopy using transmitted light and crossed polarizers. By tilting and rotating the sample in the light beam, cm-size sapphire crystals generally appeared darker than the brighter matrix (polycrystalline) grains. By observing as-fired surfaces of a sintered tube with optical microscopy and the SEM, entrapped clusters of matrix grains and "ghost grains" inside large sapphire crystals could be examined. The SEM was also used to study grain boundaries and spinel particles in samples that were sectioned and polished, preferably relief-polished, or in some cases, thermally-etched a few min. at 1550-1600°C in O_2 gas.

An SEM capable of analyzing electron beam scattering patterns (EBSP) was used to determine the orientations of sapphire crystals grown by the SSCC process on as-sintered tubes and on carefully chosen polished sections of tubes. For good EBSP images the residual surface strain in polished sapphire crystals had to be eliminated by a thermal anneal at 1100°C in air for 2h. The EBSP method was fully automated for pattern formation, acquisition and analysis. An orientation analysis required only about 5 minutes after the sample was carefully aligned to a reference crystal during setup. The atomic nature of the sapphire/PCA interface was obtained at very high magnifications and high resolution by TEM examination. Specimens were mechanically ground to a thickness of ~150 microns and then dimpled from one side to a minimum thickness of 10-20 microns. Each specimen was then ion-milled until perforation. It was very difficult to successfully thin the TEM specimens because small cracks were typically present at the single crystal/PCA interface and caused many specimens to fall apart during thinning. Finally, as mentioned above, a wet chemical analysis technique using the ICP-AES method was developed for measuring the residual concentration of MgO and codopants in heat-treated samples.

4. Results and Discussion

4.1 MgO Solubility in Al_2O_3

It was necessary to establish the solubility limit of MgO in Al_2O_3 as a function of temperature in the temperature region where abnormal growth occurred and large cm-size sapphire crystals grew in the PCA tube. It will be shown later that this information played a significant role in understanding the mechanism proposed for rapid grain-boundary migration in translucent, MgO-doped Al_2O_3.

The solubility limits (in ppm by weight) for MgO in Al_2O_3 at 1720, 1800, 1880 and 2000°C are listed in Table 3. The maximum solubility of MgO in Al_2O_3 at 1720°C was determined by the presence of spinel particles at grain boundary intersections in the microstructure of Al_2O_3 doped with 100 ppm of MgO, but no spinel particles in the composition with 50 ppm. Thus, the MgO solubility limit was set at the midpoint concentration of 75 ppm. These solubility limits at 1720 and 1800°C were surprisingly in good agreement with the data from Ando and Momoda[7] also listed in Table 3. The MgO solubility limits at 1880 and 2000°C were also determined to be midpoint MgO concentrations between sample compositions with spinel second phase and those showing only single-phase solid-solutions. In this way the solubility limits for MgO in Al_2O_3 at 1880 and 2000°C were determined as 175 and 225 ppm, respectively. It should be mentioned that the temperature of 2000°C was above the eutectic temperature of ~1975°C for the $MgAl_2O_4$ - Al_2O_3 phase diagram[8].

An example of a typical microstructure where the MgO solubility limit in Al_2O_3 was exceeded at 1800°C is given in Figure 2. The three identified particles (grains) at the 3-grain junctions were each chemically analyzed and found to contain Al, Mg and O, as shown in Figure 3A. Under similar conditions of chemical analysis, the larger matrix grains of Al_2O_3 solid solution shown in Fig. 2 contained only Al and O in their spectra (see Figure 3B). The small MgO-rich particles were assumed to be spinel based on the $MgAl_2O_4 - Al_2O_3$ phase diagram.[8]

Thermodynamics of disordered solid solutions[9] and point defect chemical reactions[10] predict a relatively simple mathematical expression, $\mathrm{Ln}\, X = a - b/T$, for very limited solubility of a solute in another solid. Here, X is the solubility in atomic fraction, T is the absolute temperature, and **a** and **b** are constants related to entropy and heat of solution[9]. The limited solubility of MgO in Al_2O_3 also follows this functionality as shown in Figure 4. The data point for MgO solubility at 2000°C was omitted

Table 3. The solubility (in ppm by weight) of MgO in Al_2O_3 at temperatures between 1700 and 2000°C.

Temperature (°C)	MgO Solubility Limit (ppm)
1720 ± 10	75 ± 25
1800	100
1880	175 ± 25
2000	225 ± 25
1700	55*
1800	95*

* Data taken from Reference 7.

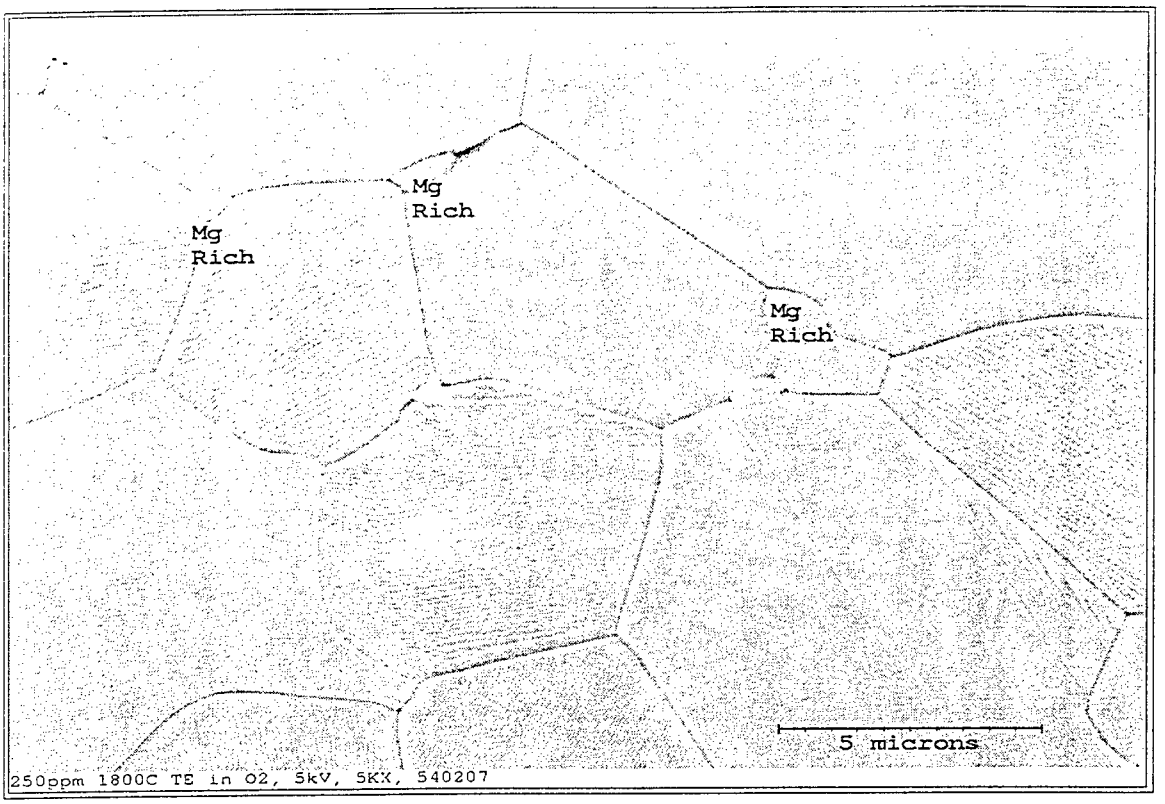

Figure 2. SEM photomicrograph of the microstructure of Al_2O_3 doped with 250 ppm MgO and equilibrated at 1800°C for 1h."Mg-rich" particles (see Figure 3) of (spinel) second phase revealed by relief-polish and thermal-etch.

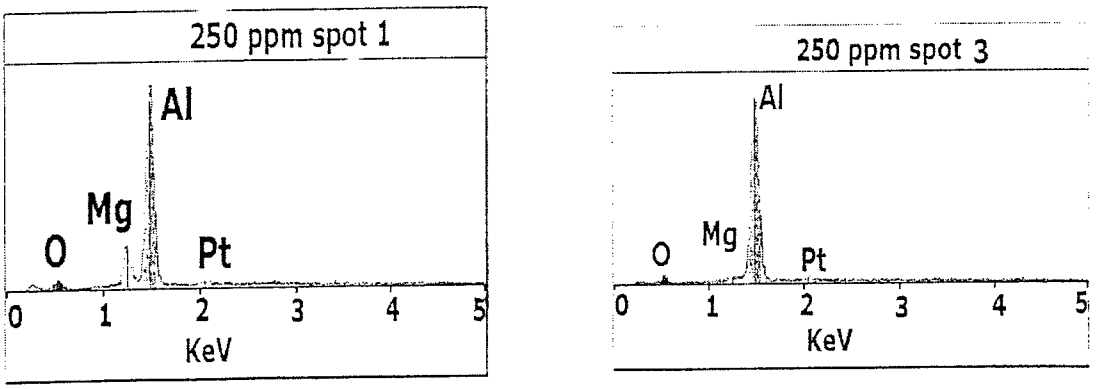

Figure 3. Spot (1) is a triple-point grain, designated in Figure 2, having a typical chemical spectrum that exhibited Mg, Al and O signals. Spot (3) is a chemical spectrum of a typical large matrix grain, showing no detection of Mg.

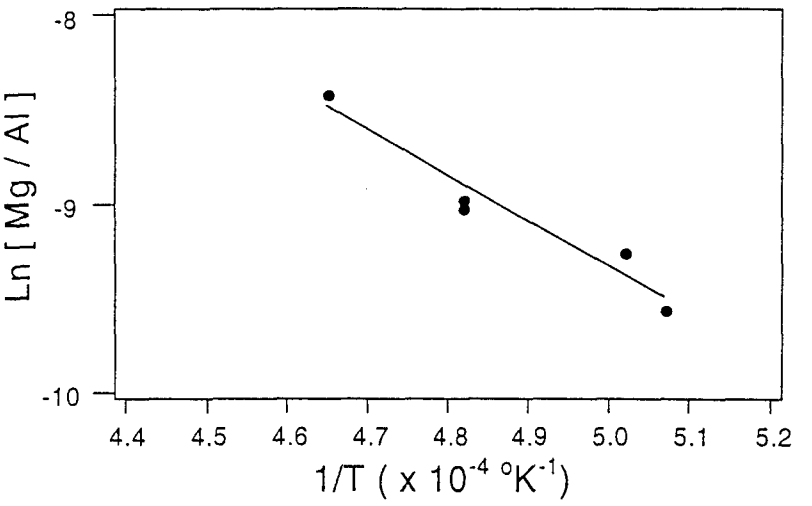

Figure 4. Natural logarithm of the solubility limit of MgO in Al_2O_3 as a function of the reciprocal of absolute temperature

because this composition was above the eutectic temperature for the $MgAl_2O_4$- Al_2O_3 system[8]. The two solubility limits measured by Ando and Momota[7] are also included in the data plotted in Figure 4. The variation of MgO solubility with temperature can be expressed by the equation,

$$\text{Ln (Mg/Al)} = 3.8 - 2.6 \times 10^4 / T \ . \qquad (3)$$

Here the term Ln (Mg/Al) represents the natural logarithm of the Mg concentration in atomic fraction. The conversion from ppm (Mg/Al) atomic fraction to ppm MgO by weight is done conveniently by multiplying the former number by the factor 0.79. For our samples prepared in moist hydrogen, the constants for entropy and heat of solution are 3.8 and 2.6×10^4, respectively. These values are relatively close to the corresponding values of 1.6 and 2.2×10^4 approximated by Ando and Momoda[8] for samples prepared in air. The constant 2.6×10^4 equals $2\Delta H/3R$[9], where ΔH is the enthalpy of solution per mole of dissolved MgO, R the gas constant (8.3 J/°K mole), and 2/3 arises from the charge neutrality condition for defects, Mg'_{Al} and $V_O^{\cdot\cdot}$, formed in the Al_2O_3 lattice. ΔH was calculated as 326 kJ/mole [3.38 eV], a very high value for MgO solubility in Al_2O_3. The MgO solubility in Al_2O_3 determined by Roy and Coble[9] was about one order of magnitude higher and in disagreement with our results presented in Figure 4.

4.2 Crystal Morphologies and Growth Variability

The morphologies of the growth fronts of sapphire crystals were primarily non-uniform and wavy when growing into the polycrystalline matrix of tube-shaped samples. Examples are illustrated in Figure 5A and B. Most large crystals initiated growth at one or both ends of tubes 7 to 10 cm in length. Figure 5A shows one large crystal abnormally grew about ¼ cm longer along the tube length in one portion than the other, whereas 5B shows two crystals, with the much larger one having a very wavy, irregular growth front. The "bright" specks located inside the growing crystals were determined to be small groups of polycrystalline matrix grain entrapped inside the rapidly growing crystals.

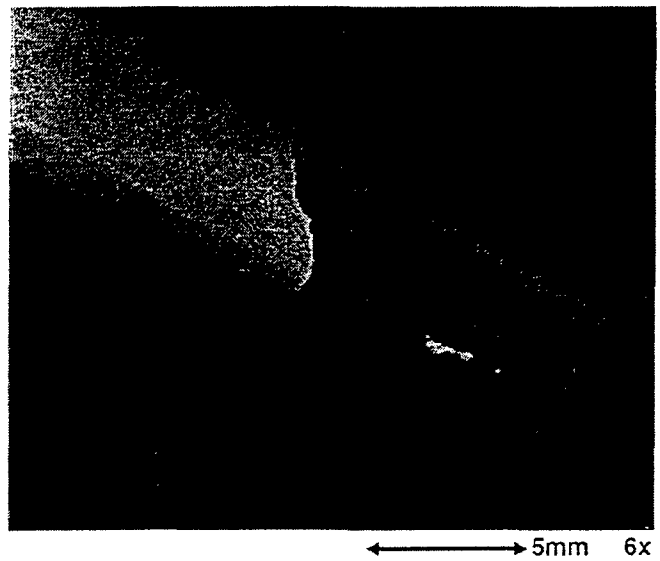

(A)

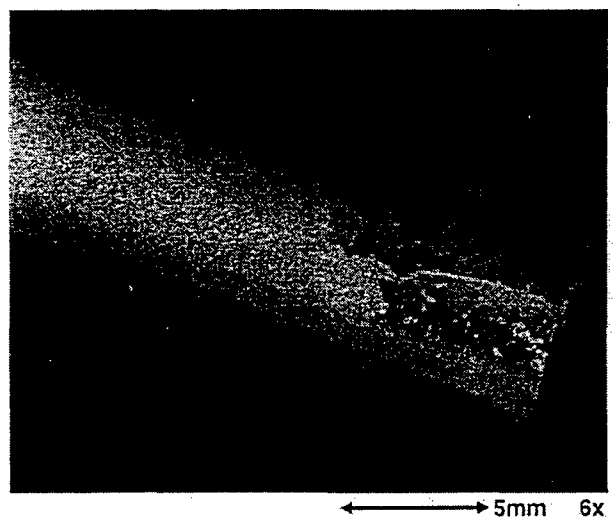

(B)

Figure 5 (A) and (B) illustrate typical non-uniform growth of large sapphire crystals starting from a tube end.

Some details of the crystal morphologies along the length and circumference of the sintered tubes are illustrated in Figure 6 for crystals actually observed. In Figure 6 the distance the crystal grew from the tube end is plotted as a function of position around the perimeter of the cylinder. In a 3h period at 1880°C the single crystal in Figure 6A grew relatively smoothly to a variable length between about 2 and 3 cm from the tube end. On the other hand, the crystal in Figure 6B grew very non-uniformly to distances ranging between about 1 and 3 cm under the same experimental conditions. By doubling the time for abnormal crystal growth at 1880°C, occasionally just two large crystals grew into a PCA tube 10 cm in length. This is shown schematically in Figure 6C for crystal 1, which grew to a distance between 5 and 7.5 cm along the length of the tube, while crystal 2 grew about 2.5 to 5 cm in length from the opposite end of the tube. Although these types of abnormal grain growth were quite useful for obtaining crystal orientations and grain boundary mobility measurements, a variety of other growth morphologies were observed. Some PCA tubes with lower MgO concentrations converted into samples having a multitude of abnormal crystals ~ ½ cm in size or just a few millimeters in size.

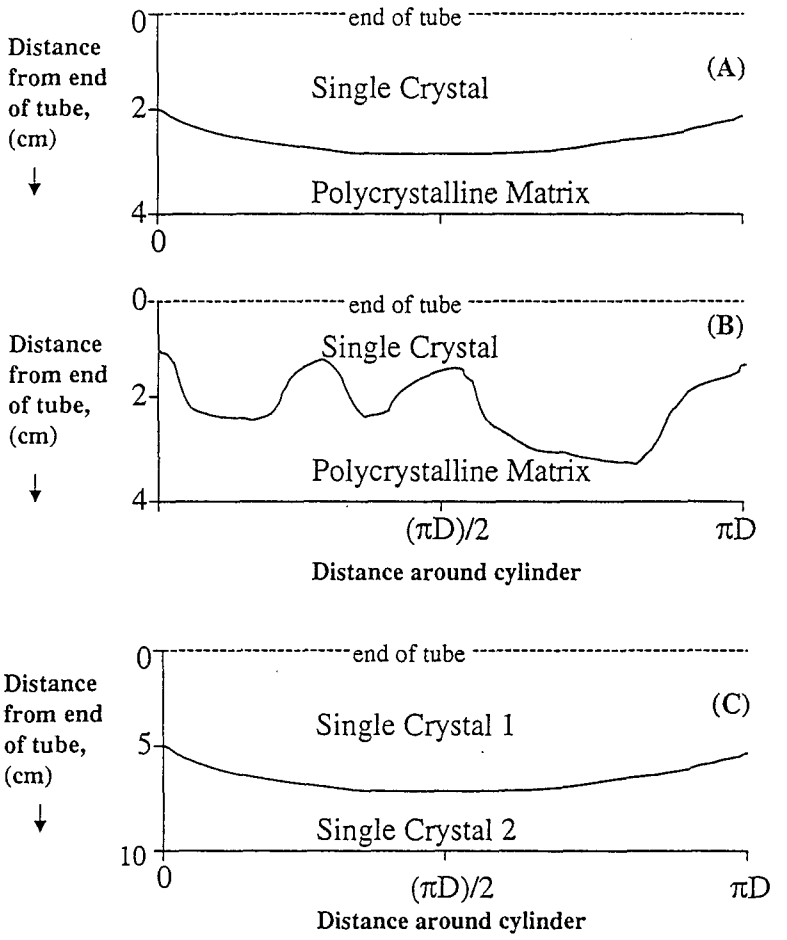

Figure 6. Schematic drawings for actual sapphire crystals grown by the SSCC process. Abnormal growth into PCA matrix from tube end with a relatively uniform growth front (A) and non-uniform growth front (B). Figure (C) illustrates two large crystals, each grown from opposite tube ends.

4.3. Characterization of the Growth Front

Some details of typical regions near the growth front at the single crystal/polycrystalline [SC/PCA] interface can be seen in Figures 7 and 8. The [SC/PCA] interface runs in a north-south direction in Figure 7. The polycrystalline grains are characterized by thermal grooves between each other and an average grain size of about 25 microns. The "whitish" region in the PCA region is caused by electron charging effects during SEM imaging. The single crystal exhibits a surface morphology revealed by a "ghost-structure" of the pre-existing grains of the PCA matrix. Once the single crystal boundary migrated through that polycrystalline region, thermal grooving between grains transformed from sharp, deep grooves into wide, shallow undulations on the surface of the growing crystal. Note the presence of singular and multiple grains of polycrystalline material entrapped within the single crystal, as observed in the upper right hand portion of Figure 7. Careful inspection of the SC/PCA interface shows it is composed of many "curved" boundary segments corresponding to neighboring grains of the polycrystalline matrix. In many regions the curved segments are still inside a PCA grain where such grains are precisely

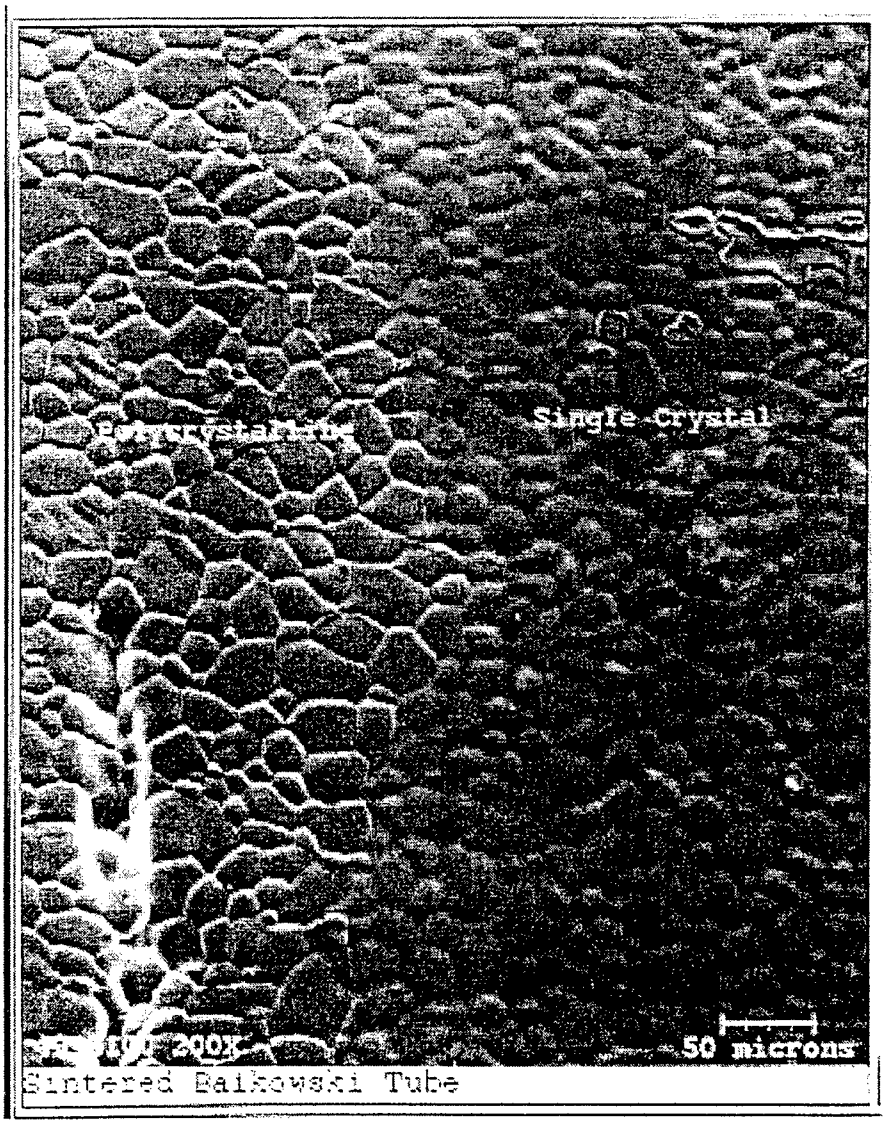

Figure 7. Typical interface between a growing single crystal and the polycrystalline matrix.

(A) (B)

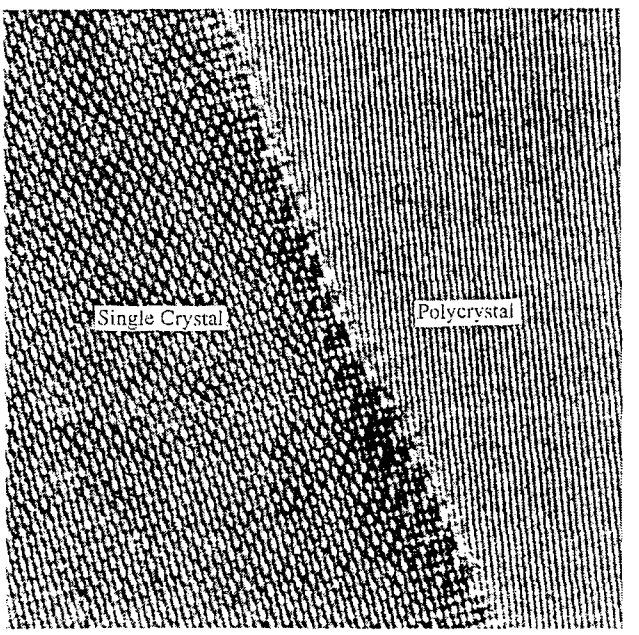

(C)

Figure 8. TEM lattice fringe images of the interfacial region between a single crystal and polycrystalline grain, (A), and between two polycrystalline grains, (B), in a sample made with Baikowski powder, doped with 350 ppm of MgO and sintered for 6h at 1880°C. Lattice fringe image (C) was taken from a similar sample doped with 350 ppm of MgO and sintered 9h at 1850°C.

in the mode of shrinkage or disappearance. There was no evidence of microscopic faceting or "straight-sided" grains at the SC/PCA interface that would indicate the presence of a liquid phase. All SC/PCA interfaces studied in this work had a similar appearance and were representative of a classical case of abnormal grain growth in the solid state.

High-resolution atomic and lattice imaging in the TEM were used to detect whether a thin layer of amorphous phase existed at the SC/PCA interface in a sample sintered for 6h at 1880°C. In Fig. 8(A) the single crystal and a neighboring polycrystalline grain were oriented in a 2-beam condition such that lattice fringe image of both grains could be observed. The lattice fringes represent the 10-14 planes of the single crystal and the 01-12 planes of the polycrystalline grain. The 2.0 nm resolution marker is also given in the photomicrograph. The lattice fringes of both grains met at the grain boundary, clearly indicating that both grains were indeed crystalline up to their interface with no evidence for a thin amorphous layer. A lattice fringe image was also taken between two polycrystalline grains near the SC/PCA interface and shown in Figure 8(B). Again, no amorphous region was observed at the grain boundary. The same TEM results were found for a different sample sintered for 9h at 1850°C [see Figure 8(C)]. In this high resolution TEM picture, the single crystal material is on the left-hand side and the polycrystalline grain is on the right. Again the lattice fringes of both grains proceed directly up to the grain interface. Furthermore, energy dispersive spectroscopy using an electron beam size of 2 nm showed no detectable difference in the composition of the single crystal, polycrystal or their interface.

4.4 Orientations of Single Crystals and Entrapped PCA Grains

The orientation of crystals in sintered tubes was determined by EBSP (electron beam scattering pattern) analysis. A sintered tube containing large (cm-size) crystals was lined up with the tube axis parallel to a major axis of the SEM microscope stage. In performing the EBSP analysis, the e-beam was placed on a portion of the tube with a tangential slope of 70° relative to the phosphor screen. The diffraction pattern on the phosphor plate was imaged by a CCD camera, collected and indexed. Once indexed, the crystallographic orientation for that point was recorded as the misorientation between the principal axes of the sample and the fixed microscope reference system. Then the stage was moved to the next crystal while keeping the stage orientation intact. In this way the orientation of all crystals analyzed was plotted on one uncorrected pole figure.

The orientation relationships of three large crystals that grew in a sintered tube 7 cm in length are shown in the c-axis pole projection given in Figure 9. This sample was initially doped with 700 ppm of MgO and sintered for 9h at 1880°C. The largest crystal, Grain 2, was ~3 cm in size and grew with its c-axis nearly perpendicular to the tube-axis. This crystal grew on the end of the tube. A top view SEM image showed that the surface of Grain 2 was highly striated topographically. A small grain from the polycrystalline matrix, labeled Mini-grain 2 in Figure 9, remained on the surface of Grain 2 and apparently resisted disappearance due to its similar orientation with Grain 2. Grains 1 and 3 were much smaller crystals, only about 1-2 cm in size, smoother in surface topology and grew with each c-axis ~ 40-46° to the tube-axis.

In another sintered tube the orientations of three large crystals were also measured by EBSP analysis. The results are plotted in the c-axis pole projection given in Figure 10. Crystals 1 and 3 grew on each tube end with each c-axis almost 90° to the tube axis. Both crystals were about 3 cm in length and had striated surface topology. Crystal 2 was about 1 cm long, smooth in surface character and grew with its c-axis ~ 45° to the tube axis.

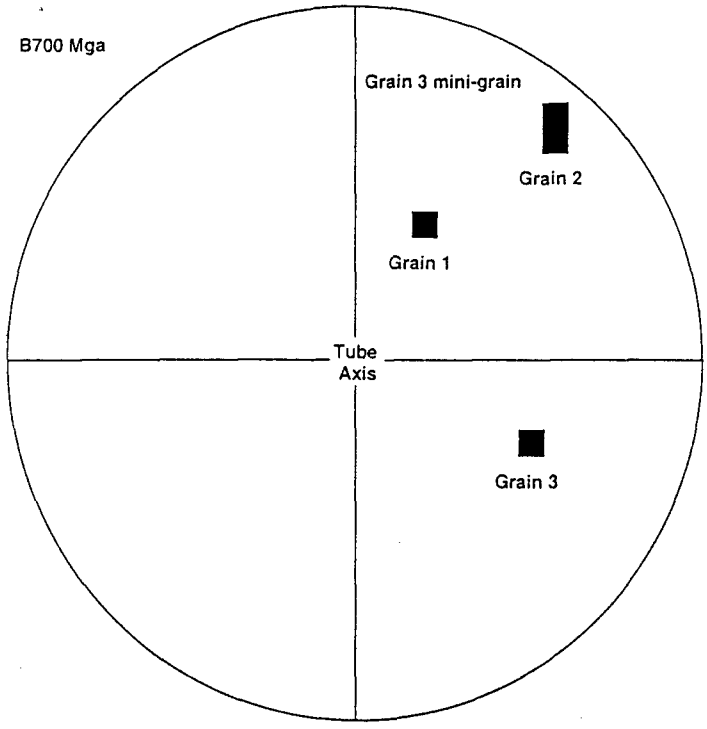

Figure 9. C-axis pole figure for sapphire crystals grown in a 7 cm tube made with Baikowski alumina initially doped with 700 ppm of MgO and sintered at 1880°C for 9h.

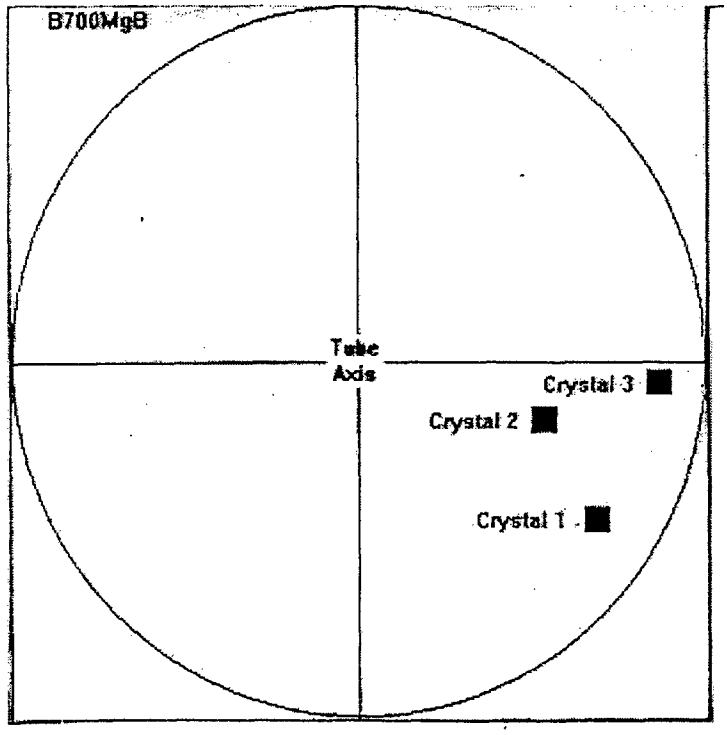

Figure 10. C-axis pole figure for sapphire crystals grown in a 7 cm tube made under the same conditions as described in Figure 9.

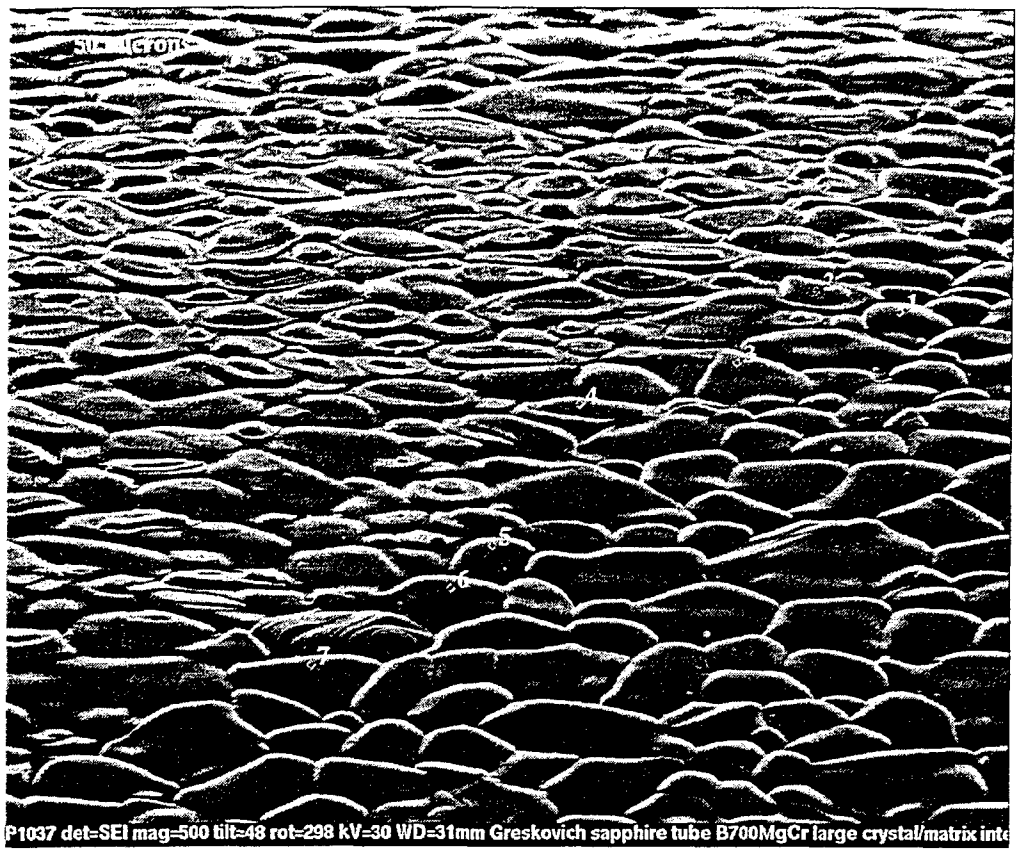

Figure 11. SEM image of single crystal/polycrystalline interface. The alumina tube was initially codoped with 700 ppm of MgO and 200 ppm of Cr_2O_3 and sintered at 1850°C for 6h.

The interfacial region between a growing single crystal and the polycrystalline matrix grains showed a peculiar topographical feature on the surface of the growing single-crystal. "Hats," or islands of randomly oriented grains, were observed on small flat facets within the single crystal matrix near the SC/PCA interface, as illustrated in Figure 11. The interface between the single crystal and the PCA matrix is difficult to discern but slopes from NE to SW, where the single crystal is on the left and the PCA grains are on the right. Grains labeled 1,3,5,6 and 7 are located just inside the polycrystalline matrix, whereas the "hat-like" islands labeled 2 and 4 are just inside the single crystal region.

The large crystal grew rapidly along its prism faces with its c-axis oriented perpendicular to the sample tube axis and retained some portions of the grains from the PCA matrix. Once the prism planes migrated quickly through the surface grains of the PCA matrix, the "hat-like" regions developed because of the slow rate of migration of the basal plane (of the newly formed portion of the single crystal) through the "stranded," misoriented surface grains. The temporary stability of the "hat-like" grain portions appears to be related to the difference in energy associated with thermal grooving of the surface grain boundaries and their disappearance after the single crystal boundary migrates through those polycrystalline grains. Careful EBSP examinations demonstrated that the "hats" were prevalent near the SC/PCA interface and the "hat-rim" facets were parallel to the basal plane of the single crystal. This was confirmed in Figure 12, where the center of the projection was the <0001> axis of the single crystal (and the "hat rim" planes were found parallel to basal plane of the single crystal). The isolated

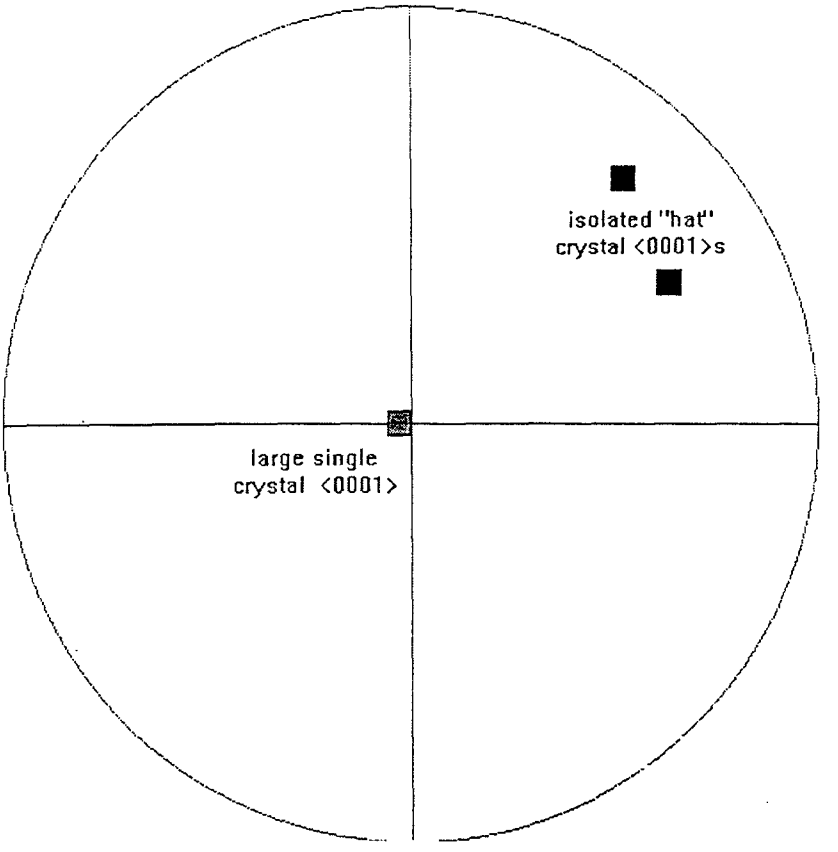

Figure 12. C-axis pole figure for a single crystal and two "hat-like" regions or islands near the SC/PCA interface. The tube axis was oriented in the east-west direction, and the center of the projection was normal to the "hat rim" facets (planes).

island grains labeled 2 and 4 in Figure 11 were found to be randomly oriented with respect to the underlying facets or single crystal, as shown in Figure 12. This information proved the island (hat-like) regions were remnants of surface grains that were on the polycrystalline tube. Therefore, the morphology of the surface grains in the PCA matrix transformed from its initial polyhedral-shape to a thin "hat"-shape island after passage of the migrating crystal boundary. With increasing time after passage of the crystal boundary, these remnant islands and mini-grains entrapped within the single crystal become smaller and smaller until they completely disappeared by mechanisms of surface diffusion and/or vapor transport.

A typical microstructure of the SC/PCA interface in the bulk sample is illustrated in Figure 13(A), where the single crystal was growing from the right-hand side. Characteristic features observed in the bulk sample near the interfacial region were isolated matrix grains entrapped inside the growing crystal (note single grain with dark-contrast) and a non-uniform interfacial front. The SC boundary migrated rapidly through the PCA matrix grains with a portion of its boundary sweeping passed the "finger-like" array or PCA matrix grains, leaving them occluded within the growing crystal. The much slower rate of grain boundary migration through the "finger-like" array of matrix grains could be caused either by a decrease in mobility of the boundary due to impurity or excess MgO segregation or by low grain boundary energy due to PCA matrix grains closely oriented with the SC. The orientation relationships

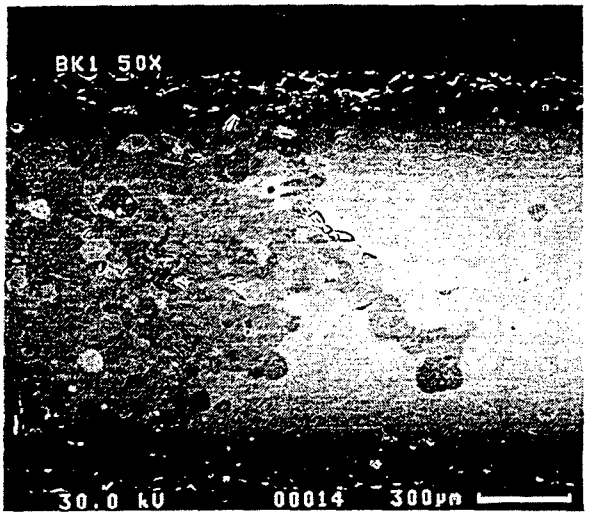

(A)

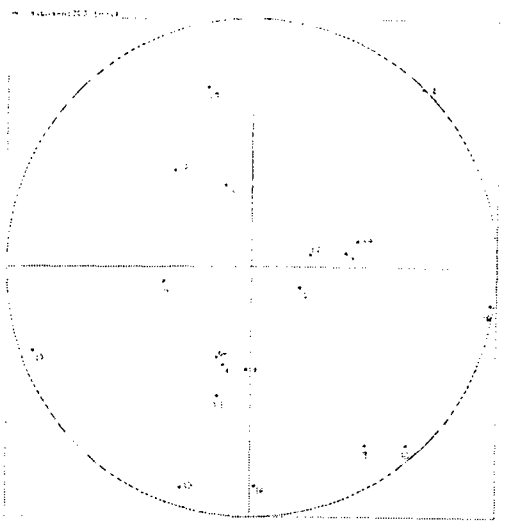

(B)

Figure 13. Bulk microstructure of the SC/PCA interfacial region (A) showing a "finger-like" array of PCA grains protruding inside the growing crystal and (B) a c-axis pole projection for 19 grains of the protruded array of grains.

between the single crystal and 19 grains in the finger-like array were studied by EBSP and plotted in Figure 13(B). The point labeled SC is the c-axis projection for the single crystal. Clearly the c-axes of the PCA grains are scattered over the stereographic projection and in general are misoriented with respect to the c-axis of the single crystal. This is strong evidence that the migration of the crystal boundary was inhibited by excess MgO in solid solution or impurities in the neighborhood of the finger-like array of PCA grains.

4.5 Factors Affecting the Abnormal Growth of Large Sapphire Grains in MgO-Doped Al_2O_3

4.5.1 Purity of Al_2O_3 Powder

A number of abnormal grain growth (AGG) experiments were done with tubes prepared with Baikowski or Sumitomo powder, similarly doped with 350 to 700 ppm of MgO, and sintered at 1800 to 1950°C in hydrogen gas with dew points between 0 and + 15°C. Under identical conditions where AGG took place in samples made with Baikowski powder, no AGG occurred in corresponding samples prepared with the higher purity Sumitomo powder. For example, AGG was observed in "Baikowski" tubes after just 3h at 1950°C while the "Sumitomo" samples doped with 350 ppm of MgO had no AGG after 9h at the same temperature. However, AGG did occur much faster in Sumitomo samples doped with lower MgO concentrations of 100 to 250 ppm. It seemed that certain impurities were responsible for the observed effect. The major impurities in the bisque-fired, extruded tubes are shown in Table 4.

Table 4. Major impurities in bisque-fired tubes made from Baikowski and Sumitomo alumina.

	Elements (in ppm)							
Sample	Na	Si	K	Ca	Ga	Y	Zn	Fe
Sumitomo AA-06	68	4	8	<1	0.2	1.1	1.5	4
Baikowski CR-10	12	20	24	<1	19	3.7	1.6	8

It is not certain what impurity in the Sumitomo sample prevented AGG at high temperatures or what impurity in the Baikowski powder stimulated AGG in samples with the same average composition and sintered under the same experimental conditions. The alkali impurities are known to evaporate from Al_2O_3 samples under reducing (hydrogen) conditions, so the different levels of these impurities may not be important. The biggest difference is the Si impurity where the concentration of Si in the Sumitomo powder is only 4 ppm and is a factor of 5 lower than that found in the Baikowski material. The differences in other impurity concentrations between these two Al_2O_3 powders are much smaller and possibly unimportant. It appears that in the presence of 350 ppm of MgO an Al_2O_3 powder with 20 ppm of Si impurity gives rise to sintered samples that undergo AGG much faster than a higher purity powder with only 4 ppm of Si. Recent SIMS analysis[11] showed that the solubility of SiO_2 in Al_2O_3 was enhanced by the presence of MgO in sintered samples of MgO-doped Al_2O_3. In light of this information, it is believed that grain boundary compositions with higher Si^{4+} and Mg^{2+} in solid solution have higher grain boundary mobility responsible for the onset of AGG.

4.5.2 Sintering Conditions and Initial MgO Concentration

During the first half of this AFOSR contract, sapphire crystals as large as 5-6 cm in length developed in tube-shaped samples that were prepared with Baikowski Al_2O_3 powder, doped with ~ 350 and 700 ppm of MgO and then sintered for long times (3 – 15h) at high temperatures (1875 – 1950°C). However, sintered samples with the same starting compositions but made from Sumitomo powder did not development cm-size crystals or undergo significant AGG. Prior work[5] on "Sumitomo" samples doped with similar MgO contents and sintered under similar conditions demonstrated that the lack of AGG was related to higher residual MgO concentrations caused by a slower rate of MgO evaporation during the sintering/grain growth process. The effort in the latter half of this AFOSR contract then focused on understanding rapid AGG by sintering Al_2O_3 compositions containing < 350 ppm of MgO.

The early stages of abnormal grain growth were observed in a series of samples made with Baikowski and Sumitomo Al_2O_3 powders doped with relatively low MgO concentrations ranging between 50 and 300 ppm. If MgO was entirely omitted from the alumina composition, samples sintered at temperatures >1700°C for more than a few hours invariably were optically opaque and contained AGG everywhere with large numbers of 0.2-1 millimeter grains. The grain growth behavior in MgO-doped samples is summarized in Table 5, where in each sample composition the largest abnormal grain was measured optically and the optical quality estimated by eye inspection. The presence of abnormal grains in the sintered microstructure was defined when the largest grain observed was greater than twice the average grain size of the PCA matrix. In general, samples containing =200 ppm of MgO sintered to various degrees of "cloudiness" where the cloudiness increased with decreasing MgO concentration and was relatively independent of sintering conditions above 1700°C. "Cloudy" samples were found to

contain large amounts of residual micron-size pores while "clear" sintered samples signified a low level of residual pores, nearly typical of translucent-grade MgO-doped Al_2O_3 used in present-day lighting applications. The results in Table 5 show that AGG was not observed in the sample compositions sintered up to temperatures of 1725°C. These microstructures consisted of a uniform grain size distribution with average grain sizes of 10 to 13 μm. The first appearance of AGG occurred in all compositions prepared with Baikowski powder that were sintered at 1740°C for 4h in hydrogen gas (dew point = +15°C). A sintered sample with 50 ppm of MgO consisted of numerous abnormal grains with sizes < 0.1 cm while the largest abnormal grain, 1.5 cm in length, grew in a sintered tube doped with 100 ppm of MgO. The size of the largest grain observed decreased from 1.5 to 0.4 cm with increasing MgO concentration from 100 to 300 ppm.. Under the same conditions the microstructures of all sintered compositions made with Sumitomo Al_2O_3 powder exhibited uniform grains of PCA with no AGG observed. A similar trend in results was also observed at sintering conditions of 1790°C for 4h for both materials with the same compositions.

By sintering at 1865°C for 3h, a large crystal 2 cm in length grew in the Sumitomo sample doped with 150 ppm of MgO. However, no AGG was observed in a Sumitomo sample doped with a higher MgO concentration of 300 ppm. Under the same conditions large abnormal grains, about 3 cm in size, developed in sintered Baikowski tubes doped with either 150 or 300 ppm of MgO. These samples also consisted of smaller abnormal grains between 0.5 and 1 cm in size and grain boundary micro-cracks here and there in the microstructure. The last set of data in Table 5 show that abnormal grains grew up to ½ to 2 mm in size in Sumitomo samples doped with ≤200 ppm of MgO but little AGG developed in the specimen doped with 300 ppm. Finally, longer sintering times of 6-10h at 1900°C caused the formation of large cm-size crystals by AGG in all Sumitomo samples doped with MgO concentrations ≤350 ppm.

4.5.3 The Dominant Role of MgO Solute Concentration

Most of the results on growth of cm-size crystals in PCA presented in Table 5 could be better understood by knowing the residual MgO concentration in sintered tubes when large (2-4 cm long) single crystals first developed. That is, once such large crystals grew during that sintering treatment, the single crystal portion or portions were selectively removed from the specimen for MgO chemical analysis. In addition, PCA samples that did not exhibit AGG but still had uniform grain size distributions were also measured for MgO concentration. The MgO concentrations were measured on samples taken from a large variety of grain growth experiments. This included samples that were (a) made with Baikowski or Sumitomo Al_2O_3 powder, (b) isothermally sintered for various times ranging from 2-12h, (c) sintered in a temperature gradient of ~14°C at temperatures between 1800 and 1900°C, and (d) co-doped with either Cr_2O_3, Ti_2O_3 or Mo. The overall results are plotted in Figure 14, showing the residual MgO concentration in samples sintered at temperatures above 1700°C in hydrogen gas. Close inspection of the data showed that growth of large single crystals by AGG did not take place in sintered Al_2O_3 containing concentrations of MgO solute > about 60 ppm. Therefore, the vertical dashed line at a "critical" MgO concentration, C_{MgO}-Crit., of ~ 60 ppm separated the single crystal region from the polycrystalline region. This was a surprising result because it was anticipated that a line (or curve) with positive slope would separate the AGG and PCA regions in this type of graph. The reasoning for a line with positive slope was simply that the MgO solubility in Al_2O_3 increases from ~ 50 ppm at 1700°C to ~ 225 ppm at 1950°C, and grain boundary mobility should increase exponentially with increased

Table 5. Effect of sintering conditions on the growth (largest-size) of abnormal grains in samples with different starting powders and MgO concentrations

Sample	MgO Content (ppm)	Largest Crystal Observed (cm)	Comments
Sintering Conditions: 1700 °C – 4h			
Baikowski	150	All PCA	Milky opaque, uniform grains [~ 8 μ]
Sumitomo	150	All PCA	Milky opaque, uniform grains [~ 8 μ]
Sintering Conditions: 1725°C – 4h			
Baikowski	150	All PCA	Milky opaque, uniform grains [~10 μ]
Sintering Conditions: 1740°C – 3h			
Baikowski	50	0.1	Cloudy sample, many abnormal grains
Baikowski	100	1.2	Cloudy sample, many abnormal grains
Baikowski	150	0.8	Slightly cloudy, fewer abnormal grains
Baikowski	300	0.4	Clear/cloudy, many regions of PCA grains
Sumitomo	100	1.0	Cloudy, many abnormal grains
Sumitomo	150	All PCA	Cloudy, and uniform grains [~10 μ]
Sumitomo	300	All PCA	Cloudy, and uniform grains [~10 μ]
Sintering Conditions: 1790°C – 4h			
Baikowski	150	0.8	Sl. Cloudy, abnormal grains [0.1cm] in PCA
Baikowski	300	0.1	Clear, abnormal grains [0.1cm] in PCA
Sumitomo	150	All PCA	Uniform grains [~22 μ]
Sumitomo	300	All PCA	Uniform grains [~ 16 μ]
Sintering Conditions: 1865°C – 3h			
Baikowski	150	3	Cloudy, some micro-cracks
Baikowski	300	3	Clear, some micro-cracks
Sumitomo	150	2	Cloudy, some micro-cracks
Sumitomo	300	All PCA	Clear, uniform grains [~ 36 μ]
Sintering Conditions: 1900°C – 3h			
Sumitomo	150	0.2	Cloudy, abnormal grains [0.04-0.08 cm]
Sumitomo	200	0.05	Sl. Cloudy, abnormal grains [0.01-0.03 cm]
Sumitomo	300	0.03	Clear & Cloudy regs., grains < 0.01 cm

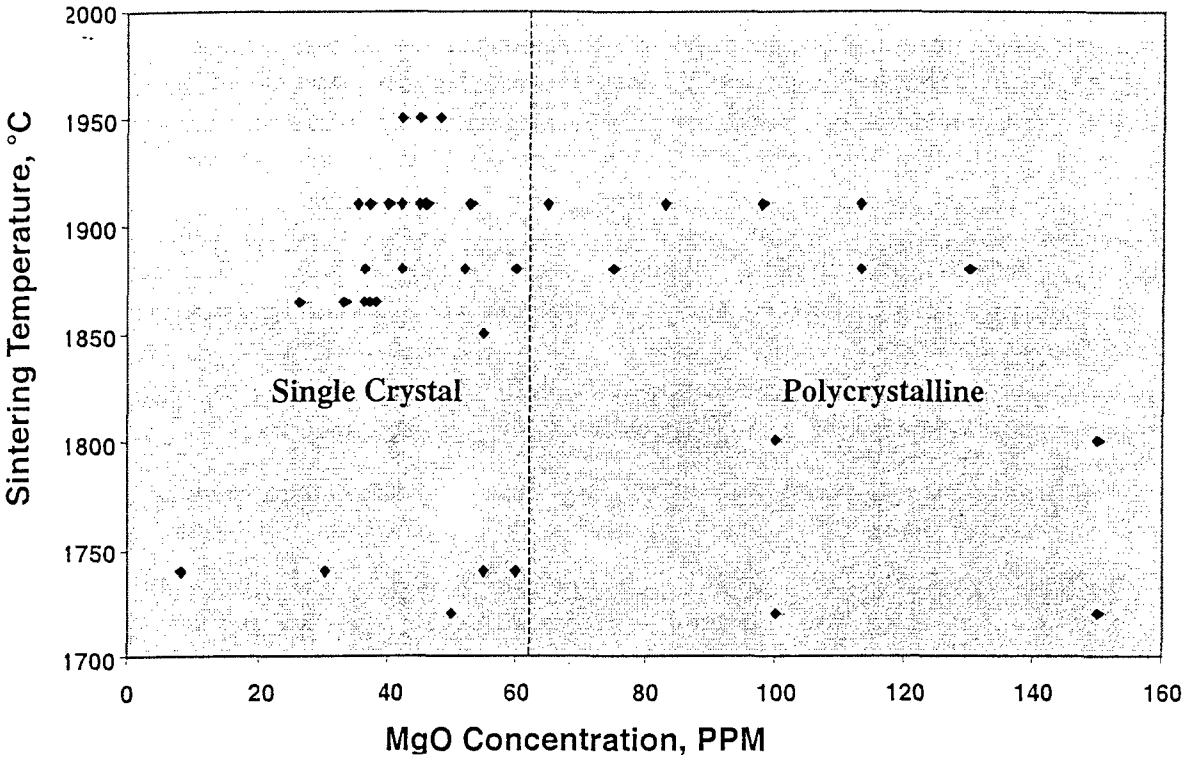

Figure 14. The residual concentration of MgO in large cm-size crystals grown in tubes sintered at various temperatures

sintering temperature for a constant MgO solute concentration (C_{MgO}). The C_{MgO}-Crit of ~60 ppm for high grain boundary mobility was well within the Al_2O_3 solid-solution region over the temperature range investigated. These observations strongly suggest that grain boundary mobility was dependent on MgO concentration within the Al_2O_3 solid-solution region and, therefore, controlled by a solid-solution mechanism. Even though powder purity and the addition of several hundred ppm of soluble co-dopants, such as Cr_2O_3 and Ti_2O_3, influenced the onset time or temperature for rapid grain boundary migration, the experimental evidence showed the grain boundary mobility was predominantly determined by the MgO solute concentration. When the MgO concentration approached ~60 ppm during grain growth, the grain boundary mobility increased drastically by about 3-4 orders of magnitude (see section 4.5.4) and cm-size crystals grew by AGG.

The mechanism is not completely understood for the sudden increase in average grain-boundary mobility at a C_{MgO}-Crit < 60 ppm in Al_2O_3 at temperatures above 1700°C. One possibility is the C_{MgO}-Crit is related and dependent on the concentration of an impurity in the alumina powders. Si-impurity is of most suspect and of special interest because its average concentration has been measured as ~ 21 ppm by weight (or 45 ppm by weight SiO_2) in sintered samples where the PCA converted into 2-3 cm-size sapphire crystals. In these same single crystals the average Mg concentration was ~ 26 ppm by weight (or 43 ppm by weight MgO). On a mole basis calculations show there is about 0.75 ppm mole Si^{4+} and 1.07 ppm mole Mg^{2+}. This means that nearly one Mg^{2+} ion is compensated by one Si^{4+} ion dissolved in the Al_2O_3 lattice when cm-size crystals begin growing abnormally in a PCA sample via the SSCC process. If true, then the "critical" MgO concentration may be controlled or dictated by

boundary mobility continues to increase slowly as the MgO concentration decreases from ~175 to about 100 ppm within the single-phase region. This means that the MgO solute in Al_2O_3 causes a strong interaction with grain boundaries and controls development of the normal grain size distributions observed in the microstructures. Since MgO evaporates from the surfaces of the sintering sample, a surface region(s) which approaches the critical MgO concentration will suddenly "nucleate" an abnormally large grain having boundaries moving with high mobility. Large abnormal grains, ranging in size between a few mm and one cm, usually form first on the tube surface near the open ends of the tube where the MgO vapor can escape the fastest. In several instances microstructures of newly grown, large (2-4 mm) grains showed these grains grew mostly laterally in the surface region (where the MgO content was < the critical value) but grew only to short depths of ~ ¼ mm where $C_{MgO} > C_{Crit.}$ Under isothermal conditions, sintered tubes 5-10 cm in length frequently contained 3 to 5 sapphire crystals that must have "nucleated" from at least 3 to 5 AGG sites along the sample surface.

As C_{MgO} decreases with continued MgO depletion from the sample, the linear relationship between V and "drag" force, F, dictates a continuing rise in V [and M_a] according to the following relationships.[13,17]

$$V = F / (1/M_o + \alpha C_{MgO}) \tag{6}$$

$$M_a = (1/M_o + \alpha C_{MgO})^{-1} \tag{7}$$

Here α is the solute interaction per unit velocity and per unit MgO concentration for restrained (normal) grain growth within the low velocity limit of boundary migration. Once C_{MgO} solute becomes slightly lower and approaches values near C_{MgO} –Crit., the localized α-value abruptly approaches very small values. The apparent mobility (see Figure 15) increases drastically by 1000-fold from about 10^{-13} to 10^{-10} m^3/Ns and approaches the value for intrinsic mobility, M_o. The spatial variability in the term, αC_{MgO}, along the SC/PCA interfacial boundary can result in higher V's at some portions of the boundary and lower V's at others. This may explain the non-uniform and wavy growth fronts observed between the single crystal and PCA regions. The groups of PCA grains often observed to be entrapped inside the rapidly growing crystal are probably due to higher values of αC_{MgO} in these localized groups. Turnbull[18] derived a theoretical expression for the intrinsic mobility of a high angle grain boundary of width, w, migrating at velocity V.

$$M_o = D_b \Omega / w k T \tag{8}$$

D_b is the appropriate grain boundary diffusion coefficient, Ω the ionic volume, and kT the thermal energy. When C_{MgO} approaches C_{MgO}-Crit., M_a increases by 1000-fold as M_a approaches M_o because of a corresponding 1000-fold increase in D_b.

The migration of a grain boundary requires simultaneous diffusion of neutral lattice ions and charged defect species, such as Al^{3+}, O^{2-}, Mg'_{Al} and $V_O^{\cdot\cdot}$, from one side to the other side of the curved boundary, assuming point defects are in thermodynamic equilibrium. In the present study on AGG in MgO-doped Al_2O_3, the observed strong effect of boundary migration velocities and mobilities on C_{MgO} solute is evidence that the grain boundary diffusion coefficient must be proportional to the concentrations of Mg'_{Al} and $V_O^{\cdot\cdot}$ defects. For defect concentrations above C_{MgO}-Crit., these charged defects probably have strong interaction energies with grain boundaries due to electric field (space charge) and strain field effects. The diffusion of O^{2-} ions is expected to be fast via the high concentration